The integron integrase efficiently prevents the melting effect of Escherichia coli single-stranded DNA-binding protein on folded attC sites.

Céline Loot, Vincent Parissi, José Antonio Escudero, Jihane Amarir-Bouhram, David Bikard, Didier Mazel

The integron integrase efficiently prevents the melting effect of *Escherichia coli* SSB protein on folded *attC* sites

Céline Loot[1], Vincent Parissi[2], José Antonio Escudero[1], Jihane Amarir-Bouhram[1], David Bikard[1] and Didier Mazel[1#]

[1]Institut Pasteur, Unité Plasticité du Génome Bactérien, CNRS UMR3525, 75724 Paris, France.

[2]Laboratoire MCMP, UMR 5234 CNRS-Université Victor Segalen Bordeaux 2, 33076 Bordeaux, France.

[#]Correspondent footnote: mazel@pasteur.fr

Tel : +33 1 4061 3284

Fax : +33 1 4568 8834

Running title: Regulation of *attC* site folding

Abstract

Integrons play a major role in the dissemination of antibiotic resistance genes among bacteria. Rearrangement of gene cassettes occurs by recombination between *attI* and *attC* sites, catalyzed by the integron integrase. Integron recombination uses an unconventional mechanism involving a folded single-stranded *attC* site. This site could be a target for several host factors and more precisely for the proteins able to bind single-stranded DNA. One of these, the *Escherichia coli* Single-Stranded DNA-binding protein (SSB), regulates many DNA processes. We studied the influence of this protein on integron recombination. Our results show the ability of SSB to strongly bind folded *attC* sites and to destabilise them. This effect is observed only in absence of the integrase. Indeed, we provided evidence that the integrase is able to counterbalance the observed effect of SSB on *attC* site folding. We showed that IntI1 possesses an intrinsic property to capture *attC* sites at the moment of their extrusion, stabilizing them and recombining them efficiently. The stability of DNA secondary structures in the chromosome must be restrained to avoid genetic instability (mutations or deletions) and/or toxicity (replication arrest). SSB, which hampers *attC* site folding in the absence of the integrase, likely plays an important role in maintaining the integrity, and thus

the recombinogenic functionality of the integron *attC* sites. We also tested the RecA host factor and excluded any role of this protein in integron recombination.

Introduction

Integrons have been isolated on mobile elements responsible for the capture and dissemination of antibiotic resistance genes among Gram negative bacteria (1). More recently, their importance has been highlighted by the discovery of integrons in the chromosomes (chromosomal integrons) of environmental strains of bacteria (2). This has led to the extension of their role from acquisition of resistance genes to a wider role in the adaptation of bacteria to different environments (3). The discovery that integron recombination was controlled by the SOS response has further connected these elements to bacterial adaptive responses (4). Integrons are composed of three key elements: an integrase gene (*intI*), which encodes a tyrosine (Y) recombinase performing the site-specific recombination (SSR) reaction, a primary recombination site (*attI*), where the incorporation of gene cassettes occurs, and a strong resident promoter (Pc) (5). Gene cassettes are devoid of promoters and mostly correspond to genes associated with an *attC* recombination site. The *attC* X *attI* recombination event catalyzed by IntI leads to cassette integration at the *attI* site, downstream of the Pc promoter allowing gene cassette expression (6). IntI can also catalyze recombination between two consecutive *attC* sites leading to cassette excision.

The structures of *attI* and *attC* sites differ significantly from the canonical Y-recombinase core sites (for review see (7)) and integron site-specific recombination is described as an atypical mechanism, in comparison to the classical SSR largely used in bacteria for movement of mobile genetic elements such as prophages or genomic islands (8).

The major distinctive characteristic of integron SSR comes from the properties of the *attC* sites. Indeed, it has been previously shown that the *attC* site recombines as a single-stranded (ss) DNA folded structure, in contrast to the *attI* site, which is recombined in a double-stranded (ds) form (9). The length of natural *attC* sites varies from 57 to 141 bp. They include two regions of inverted homology, R"-L" and L'-R', separated by a central region that is highly variable in length and sequence (Figure 1A) (10). In contrast with the heterogeneity of their sequences, *attC* sites display a strikingly conserved palindromic organization (11) that can form secondary structures through DNA strand self-pairing (Figure 1B). Upon folding, ss *attC* sites show a structure resembling a canonical core site consisting of R and L boxes separated by an unpaired central segment (UCS), two or three extrahelical bases (EHB) and a

variable terminal structure (VTS), (12). The VTS varies in length among various *attC* sites, from 3 predicted unpaired nucleotides such as for $attC_{aadA7}$, to a complex branched secondary structure in the larger sites such as VCR (*Vibrio cholerae* repeat) sites (Figure 1B).

It has been shown using a DNA binding assay that IntI1 binds strongly and specifically to the bottom strand (bs) of ss *attC* DNA (13). *In vivo*, it has also been shown that only the bs of the *attC* site is used as a substrate during gene cassette integration (9) thereby creating an atypical Holliday junction (aHJ) between the ss *attC* and the ds *attI* site. We recently proved the implication of replication in the resolution of the aHJ and definitively ruled out the involvement of a second strand exchange of any kind in the *attC* x *attI* reaction (14).

We have previously shown that cellular bacterial processes delivering ssDNA, such as conjugation and replication, favor the proper folding of *attC* sites (Figure 1C, "ssDNA pathway" (1)), (15), (14). By developing a very sensitive *in vivo* assay, we also provided evidence that *attC* sites can recombine as cruciform structures by extrusion from double-stranded DNA (Figure 1C, "dsDNA pathway" (2)), (14). Moreover, we showed an influence of DNA superhelicity on *attC* site extrusion and recombination *in vitro* and *in vivo* (14). We demonstrated that the proper folding of *attC* sites depends on both the propensity to form non-recombinogenic structures and the length of their variable terminal structures (VTS).

Since integron recombination uses *attC* sites in a single-stranded form, the host cell factors which have affinity towards single-stranded DNA can potentially regulate integron recombination by acting on *attC* sites, impairing their folding and/or impeding the integrase activity.

In this paper, we examine the effect of several of these specific host factors on *attC* site folding. Among them, we chose to investigate the effect of single-stranded DNA-binding proteins SSB and RecA.

Escherichia coli Single-Stranded DNA-Binding Protein (SSB) is essential for cell viability (16). During replication, SSB binds tightly and cooperatively to ssDNA to prevent premature annealing. Indeed, the single-stranded DNA has a natural tendency to revert to the double-stranded form, but SSB binds to the single strands, keeping them separate and allowing the DNA replication machinery to proceed (for review see (17)). In addition, SSB is implicated in several other cellular processes, such as homologous recombination, mismatch repair and excision repair (for review see (16)). Moreover, recent studies found that SSB is not static when bound to DNA but could migrate randomly on single-stranded DNA. Indeed, SSB diffusion can melt short DNA hairpins and by consequence remove these secondary structures spontaneously formed by DNA (18). This function is biologically important because RecA,

which is necessary for recombinational DNA repair, does not bind well to secondary structures formed in ssDNA. SSB, through its ability to destabilize the intramolecular DNA basepairing within ssDNA, allows RecA to form a contiguous filament on the DNA (19).

RecA, a multifunctional DNA-binding protein with ubiquitous distribution in nature, plays a central role in both homologous recombination and post-replicative DNA repair mechanisms (see above). In bacteria, it also plays a role in the SOS response as a co-protease for the autocatalytic cleavage of the LexA repressor leading to de-repression of the SOS regulon genes (20). The RecA protein binds strongly, and in long clusters, to ssDNA to form a nucleoprotein filament.

Since integron recombination uses a folded single-stranded *attC* site, we hypothesized that SSB could potentially act on the folded *attC* site and ultimately on integron recombination. SSB could bind parts of the folded *attC* that remain as single-stranded DNA (i.e. UCS and/or VTS, see Figure 1B), thus destabilizing/unpairing recombinogenic *attC* structures and impeding integrase activity. We also studied the role of RecA in integron recombination.

By using a gel retardation assay, we showed that SSB can bind folded *attC* sites. Moreover, a replication slippage assay allowed us to conclude that this binding induces the destabilization of *attC* site folding *in vivo*. Interestingly, this effect of SSB is not observed in the presence of the integron integrase. We also provide evidence that, contrary to SSB, IntI1 possesses an intrinsic property to capture *attC* sites at the moment of their extrusion, stabilizing and recombining them efficiently.

The stability of secondary structures in the cell must be limited to avoid genetic instability (mutations or deletions) and/or toxicity (replication arrest). SSB is able to restrain the formation of *attC* secondary structures in the absence of the integrase, ensuring the integrity of integron *attC* sites when recombination is not happening. We also demonstrated that, when expressed, the integrase is able to counterbalance this effect of SSB even when SSB is over-expressed.

By using a set of similar experiments, we demonstrated that RecA does not regulate integron recombination.

We conclude that the interplay between SSB and the *attC* sites represents another example of host regulation of *attC* site folding.

Materials and Methods

Bacterial strains, plasmids, oligonucleotides and media

Bacterial strains, plasmids and oligonucleotide primer sequences are described in Tables S1, S2 and S3. *Escherichia coli* strains were grown in Luria Bertani broth (LB) at 37°C. Antibiotics were used at the following concentrations: ampicillin (Ap), 100 µg/ml, chloramphenicol (Cm), 25 µg/ml, kanamycin (Km), 25 µg/ml, spectinomycin (Sp), 50 µg/ml and tetracyclin (Tc), 15 µg/ml. Diaminopimelic acid (DAP) was supplemented when necessary to a final concentration of 0.3 mM. Glucose and L-arabinose were added at a final concentration of 10 and 2 mg/ml respectively. Chemicals were obtained from Sigma-Aldrich (France).

Integron cassette excision assay

SSB over-expression assay

The two plasmids pBAD::*intI1* (p7383, Km^R) and pHYD620 (p7305, Sp^R, which carries the *ssb* gene on a pSC101 vector; approximately 5 copies/cell), were introduced by transformation into a MG1655 Δ*dapA* derivative strain which contains an insertion (in the attB lambda site) of a plasmid carrying a *dapA* gene interrupted by the two specific *attI1* and $attC_{aadA7}$ sites (pB117, ωB768, ωC021, see Table S1 and S2), $attC_{aadA7}$ and $attC_{ereA2}$ sites (pB647, ωB661, ωB726) and *attI1* and *attI1* sites (pB119, ωB662, ωB735). These strains are unable to synthesize DAP (2, 6-diaminopimelic acid), and as a result are not viable without DAP supplemented in the medium. Recombination between *att* sites causes excision of the synthetic cassette, restoring a functional *dapA* gene and allowing the strain to grow on DAP-free medium. As controls, we also transformed this MG1655Δ*dapA* strain with the previously used pBAD::*intI1* plasmid and with the control vector pCL1920 devoid of the *ssb* gene (p8008, Sp^R, ωC020, ωB725, ωB734). We also transformed MG1655Δ*dapA* strains by pCL1920 or pHYD620 but without pBAD::*intI* (ωC018, ωC019, ωB723, ωB724, ωB732 and ωB733).

After overnight growth in the presence of appropriate antibiotics (Sp, Cm and Km), DAP and 1% glucose, strains were cultivated for 6h in the presence of 0.2% arabinose to allow *intI1* expression and plated on agar containing either LB or LB+DAP. Recombination activity is calculated as the ratio of the number of cells growing in the absence of DAP over the total number of cells.

RecA over-expression assay

In order to test RecA over-expression in the integron cassette excision assay, we processed exactly as in the SSB over-expression assay but transformed pGB2-ara-$RecA_{Eco}$ (pB981, Sp^R,

which carries the *recA* gene on a pSC101 vector) in place of the pHYD620 (ωC071, ωC069, ωB720, ωB722, ωB729, ωB731) and the control vector pGB2 (pB495), in place of pCL1920 (ωC070, ωC068, ωB719, ωB721, ωB728, ωB730).

ssb-200 and *recA269::tn10* assays

In order to test the effect of SSB and RecA inactivation in the integron cassette excision assay, we proceeded exactly as in the SSB and RecA over-expression assays (described above). pBAD::*intI1* (p7383, Km^R) was introduced by transformation into MG1655Δ*dapA* , MG1655Δ*dapA ssb-200 and recA269::tn10* derivative strains which contain an insertion (in the attB lambda site) of a plasmid carrying a *dapA* gene interrupted by the two specific *attI1* and $attC_{aadA7}$ sites (pB117, ωB768, ωB769, ωB149, ωB848, ωB849, ωB645, see Table S1 and S2), $attC_{aadA7}$ and $attC_{ereA2}$ sites (pB647, ωB661, ωB771, ωB660, ωB718, ωB851, ωB717) and *attI1* and *attI1* sites (pB119, ωB662, ωB770, ωB150, ωB727, ωB850, ωB646).

Replication slippage assay

To determine reversion frequencies, 100 ml of *E. coli* GJ1885 and GJ1890 strains (ω6737 and ω6738), transformed by the pBR derivative plasmids (p5087, p5088, p6671, p6672, p8558 and p8559), were grown up to OD_{600}=0.8 in LB medium containing ampicillin from 4 ml of an overnight culture. Reversion frequencies are calculated as the number of Cm^R cells in the population, which is determined by plating the equivalent of 90 ml of cells on medium containing ampicillin and chloramphenicol. Total viable cells were determined by plating on medium containing ampicillin. The frequency represents the mean of 4 independent experiments. The partial or complete deletion of the *attC* site was confirmed for several Cm^R reversion events by sequencing. To study the effect of the integrase on reversion frequency, we performed the same experiment by employing the previously used GJ1885 and GJ1890 strains. We transformed them with the pBAD::*intI1Y312F* plasmid (Sp^R, p8741). To determine reversion frequencies, 100 ml of these strains (ω8749, ω8752 and ω8755) were grown up to OD_{600}=0.8 in LB medium containing ampicillin and kanamycin with 1% glucose (integrase gene repression) or 0.2% arabinose (integrase gene expression) from 4 ml of an overnight culture.

Protein purification

Bacterial strain BL21(DE3)plysS (21) was transformed with pET-derived plasmids expressing the His-IntI integrase (p4634, ωC004). The protein purification was carried out as

204 described by Johansson and collaborators (22) and with the minor modifications described by
205 Demarre and collaborators (23). The *E. coli* Single-Strand Binding protein (SSB) is provided
206 from Sigma (product code **S3917**).
207
208 ***Electrophoretic mobility shift assay (EMSA)***
209 The SSB proteins were incubated with 0.6 pmol of P^{32}-labeled DNA oligonucleotides
210 corresponding to the bottom strands of the wild type (o32), the synthetic paired (o42) or the
211 synthetic unpaired $VCR_{2/1}$ site derivative (o36, see Table S3). The EMSA was carried out as
212 described by Frumerie and collaborators (24). Quantifications were made using Image Gauge
213 version 4.0.0 (FUJI Photo Film Co. Ltd), manually defining the lanes and using the automatic
214 peak search function. All other functions were at default values.
215
216 **attC *site folding assay***
217
218 The 100 bp ds *att*I1 containing fragment was generated by annealing the attI1-F
219 oligonucleotide with the complementary attI1-R oligonucleotide. The 120 bp ds *aadA7*
220 fragment was obtained by PCR amplification using the p4136 vector as template and aadA7-F
221 and aadA7-R primers. The 131 bp ds VCR fragment was obtained by PCR amplification
222 using the p1880 vector and VCR-F and VCR-R primers. The 119 bp ds *aadA7* mutant
223 fragment was obtained by PCR amplification using the p4250 vector as template and aadA7-F
224 and aadA7-R primers.
225 Under standard conditions the melting temperature of a 50 µg/ml solution of each fragment is
226 measured as the OD_{260nm} in a thermostatic spectrophotometer at 37°C. Fragments are pre-
227 chilled to 4°C and pre-heated to 95°C. To analyze the effect of IntI1, proteins are added to the
228 fragment solution 30 min after the beginning of the measurement. The OD_{260nm} measurement
229 of the proteins alone was previously performed and subtracted from the measurement
230 obtained in the mixture in order to determine the accurate values of the fragment solution.
231
232 **Results**
233
234 ***SSB binds folded* attC *sites***
235 It has been shown that single-stranded DNA-binding protein, SSB, destabilizes secondary
236 structures in ssDNA during major cellular processes such as DNA replication, repair, and
237 homologous recombination (25) (19), (26). We therefore hypothesized that SSB can bind

folded *attC* sites and destabilize them. To determine if this was the case, we investigated the binding capacity of SSB on folded *attC* sites using an electrophoretic mobility shift assay (EMSA). In order to mimic the *attC* site's bottom strand (bs), we used VCR_dbs substrate, a single-stranded oligonucleotide of ~90 bases containing a shorter version of the $VCR_{2/1}$bs site (23). In this substrate, the central part of the site (VTS) was removed and substituted with GAA (VCR_dbs, Figure 2A), a modification previously described and shown to be fully recombinogenic (23).

As controls, we constructed two other synthetic *attC* sites, namely the unpaired and paired VCR_dbs sites derivative. To obtain fully paired VCR_dbs site derivative, we introduced specific mutations in the unpaired strand parts of the folded VCR_dbs site in order to introduce complementarity and pair them. Finally, to obtain the unpaired VCR_dbs derivative, we introduced specific mutations in the double-stranded parts of the folded VCR_dbs site in order to unpair them (Figure 2A).

The results from EMSA are presented in Figure 2B. In the presence of SSB, distinct shifted bands (I and II), corresponding to SSB-DNA complexes, can be seen for both VCR_dbs and unpaired VCR_dbs sites derivative. Bands I and II probably correspond to different SSB-binding modes and/or different types of intertetramer cooperativity (see Discussion). As expected, for the paired VCR_dbs derivative, we failed to observe distinct and significantly shifted bands. The band intensities on the gels were quantified, confirming the ability of SSB to bind single-stranded parts of *attC* sites very efficiently (Figure 2C). We observed, among free DNA, higher electrophoretic migration bands in the VCR_dbs and paired VCR_dbs derivative lanes. Note that these supplementary bands probably correspond to DNA dimer formation favored by the presence of inverted repeats. The presence of these DNA dimers does not alter the interpretation of the results.

SSB destabilizes folded* attC *sites

We hypothesized that the consequence of SSB binding on the folded *attC* sites could be a destabilization effect. Indeed, Reddy and collaborators have previously shown the ability of SSB to efficiently and rapidly bind stem loops, melting these secondary structures and facilitating the binding of RecA (26). To study this, we developed a replication slippage assay. Indeed, a direct correlation between the stability of secondary structures and the frequency of replication slippage has already been demonstrated (27). The model proposed is that the formation of a stem-loop structure between a pair of flanking direct sites during replication permits a slippage event. This results in precise or nearly precise loss of the

structured region. As SSB is essential in *E. coli*, the slippage assays were performed in the wild type SSB context or in an *ssb-200* mutant. The *ssb-200* mutation corresponds to a G > A substitution at nucleotide 41 resulting in an amino acid substitution at position 4 (G4D). This mutation induces a *tex* (transposon excision) phenotype leading to an increase in the precise excision frequency of a Tn10 derivative (Tn10dKan) (28). Interestingly, Reddy and collaborators showed that *tex* mutant *ssb-200* was not affected in any other functions mediated by SSB, such as replication, recombination, or repair. This suggests that the observed *tex* phenotype of this mutant is probably only due to an incapability of the SSB-200 protein to destabilize stem loop structures formed by the inverted repeats of the Tn10dKan. Thus if the previously observed binding of SSB on the *attC* folded sites induces their melting, it is very likely that such an effect would not be observed with SSB-200.

We constructed a pBR325 derivative plasmid carrying an $attC_{aadA7}$ site inserted in the *cat* resistance gene, in such way that the loss of this *attC* site by "replication slippage" would lead to the reconstitution of a functional *cat* gene (p5087, see Materials and Methods and Figure 3A). This plasmid was transformed into an *ssb-200* mutant strain (ω6738, from (28) and in its *ssb*-wt parental strain GJ1885 (ω6737). The Cm^R reversion frequency obtained for the parental strain was $5.5x10^{-11}$. Interestingly, the frequency of reversion for the *ssb-200* strain was approximately fourteen fold higher ($7.6x10^{-10}$) (Figure 3B). Note that several of the Cm^R clones were sequenced in order to confirm deletion of the *attC* sites (see *attC* deletion frequencies, Figure 3B). These results suggest that SSB protein reduces the *attC* site loss mediated by replication slippage events, probably by binding and destabilizing the single-stranded folded *attC* site. To confirm that the obtained frequency of replication slippage is not influenced by the local context (transcription, replication, nucleotide sequences), we performed a set of experimental controls. *attC* sites were cloned into further pBR derivatives in both orientations within the *cat* resistance gene. Moreover, the *cat* gene was cloned in both orientations on the plasmid (see Materials and Methods). In all cases we obtained the same order of Cm^R reversion frequencies for the four tested constructions in the *wt* context and in the *ssb-200* context (data not shown, see Materials and Methods, Table S1 and S2). As an additional control, we constructed a synthetic derivative of $attC_{aadA7}$ site presenting a lower free energy of single-stranded *attC* site folding (ΔG= -5.1 kcal mol^{-1}) than the natural $attC_{aadA7}$ site (ΔG= -19.1 kcal mol^{-1}). For this, we introduced specific mutations in the double-stranded parts of the natural $attC_{aadA7}$ site in order to unpair them. We called this synthetic *attC* site an unpaired $attC_{aadA7}$ site derivative (Figure 4A). As with the $attC_{aadA7}$ site, we also observed a decrease in *attC* deletion frequencies in the *ssb-200* context (~13-fold, ω8609)

compared to the *wt* context (ω8605) (Figure 4B). This result shows that the probable destabilization effect of SSB is not only on the *attC* sites, but more generally on single-stranded folded secondary structures. We also cloned the unpaired $attC_{aadA7}$ site derivative in the opposite orientation within the *cat* resistance gene and we obtained the same order of Cm^R reversion and *attC* deletion frequencies for this construction in both the *wt* context (ω8604) and in the *ssb-200* context (ω8608, data not shown).

Altogether, these assays confirmed that SSB can destabilize folded *attC* sites in a non-specific manner.

The integrase stabilizes* attC *site folding

We showed a destabilizing effect of SSB on folded *attC* sites, in the absence of integrase. As the integrase likely stabilizes the folded *attC* structure, we could expect this effect to be counterbalanced in presence of this protein. In order to test this hypothesis, we assessed the effect of IntI1 expression on the slippage frequency in the previously described assay. We introduced in the GJ1885 strain (ω6791), the p8741 plasmid carrying the *intI1* gene under the control of the inducible P_{bad} promoter (ω8749). We chose to use an *intI1* gene mutated for the catalytic tyrosine (Y312F) in order to observe the effect of IntI1 binding without being influenced by potential recombination events that could occur between copies of the plasmid. It has been previously shown that when substituting the reactive nucleophilic tyrosine with the inert phenylalanine (IntI1Y312F), the ability of the integrase to attack the DNA was lost, but the *attC* site binding capability was preserved (22). The results showed that in the IntI1Y312F expression context (arabinose induction, +) the Cm^R reversion and *attC* deletion frequencies are 25-fold higher than in the absence of the integrase (glucose repression, -) (Figure 3B and 4C). This suggests that IntI1, contrary to SSB, increases the *attC* site loss mediated by replication slippage events, probably by stabilizing folded *attC* sites. To confirm that this observed stabilizing effect of IntI1 on *attC* folding is specific to *attC* sites, we performed the same experiment by using the previously used unpaired $attC_{aadA7}$ derivative (Figure 4A) which theoretically lost its IntI1-binding boxes (ω8752). As expected in this case, we obtained a very low and probably non-significant stabilizing effect of IntI1 (6-fold higher) compared to the wild type $attC_{aadA7}$ site (25-fold higher, Figure 4C). We demonstrated here that the integron integrase stabilizes the folding of *attC* sites in a specific manner.

In vitro *study of IntI1 and SSB on* attC *site folding*

In order to specify the effect of the integrase on *attC* site folding, we performed additional *in vitro* experiments. Indeed, it has been shown that IntI1 possesses the intrinsic property to efficiently catalyze strand transfer *in vitro* between *attC* fragments in the absence of other bacterial proteins, suggesting the ability of the integrase to favor the *attC* site folding or to stabilize it (29), (30). To confirm this observation, we set up an *in vitro* folding assay allowing us to easily monitor the single-stranded or double-stranded folding of short DNA fragments containing *attC* sites. The OD variations, measured at 260 nm (OD_{260}), directly reflect the DNA hybridization modifications. Indeed, OD_{260} is comparatively lower when the DNA fragment is in the double-stranded (ds) form rather than in the single-stranded (ss) form. The pre-heated $attC_{aadA7}$ fragment led to an OD_{260} close to 1.2 corresponding to the fully ssDNA form of the fragment (red curve, Figure 5A) and the pre-chilled $attC_{aadA7}$ fragment led to an OD_{260} close to 0.6 corresponding to the fully dsDNA form (blue curve, Figure 5A). By stabilizing the temperature to 37°C, the OD_{260} of the pre-heated fragment decreased to 0.9 corresponding to the partially dsDNA form of the fragment. We also obtained the same partially dsDNA structure from the pre-chilled fragment. These results were also reproduced using the $VCR_{2/1}$-containing fragments (Figure 5B) but not for *attI1* sites (site not forming hairpin structure, Figure 5C). This confirms that *attC* sites share a common partially dsDNA form, in contrast to *attI1* which remains fully double-stranded. Addition of IntI1 to both pre-chilled and pre-heated $attC_{aadA7}$ (Figure 5A) and $VCR_{2/1}$ (Figure 5B) fragments led to an OD_{260} close to 1.2, suggesting that the enzyme favors the formation of the fully single-stranded folded *attC* site and stabilizes this structure. In contrast, no such effect was found using the *att1I* site, suggesting that this activity of IntI1 is highly specific to *attC* sites. As a supplementary control, we tested a mutated $attC_{aadA7}$ site (Figure 5D) where the extrahelical G base has been deleted in order to prevent the specific binding of IntI1 on the L box (Figure 1B) (22). As expected, by using this mutated site, we failed to observe any influence of IntI1 on *attC* site folding highlighting the specificity of the IntI1 proprieties for the *attC* sites.

Interestingly, when SSB is used instead of IntI1, perturbation of the fragments' folding was only observed on pre-heated DNA. This suggests that the protein binds the single-stranded fragments and keeps it in a single-stranded form (Figure 6A and 6B) and does not intervene in the *attC* folding property as observed with IntI1. This also highlights the specificity of the effect observed with IntI1 confirming that the folding effect was due to an intrinsic property of the enzyme to favor and stabilize the folding of DNA strands, and not to an unspecific DNA avidity.

In conclusion, while both SSB and IntI1 proteins bind the folded *attC* site, the consequences of their binding would be antagonistic, since SSB seems to destabilize the folded *attC* site, while IntI1 assits with *attC* site folding.

SSB does not modulate integron recombination

We tested the recombination of *attC* sites in conditions of SSB over-expression and in a *ssb-200* mutant context. We used the excision assay described in (31). This assay allows us to directly measure *attC* recombination through restoration of the *dapA* reading frame. We inserted in a MG1655Δ*dapA* strain a plasmid containing a *dapA* gene interrupted by two specific recombination sites, *attI1* and $attC_{aadA7}$ (Figure 7A, ωB768), $attC_{aadA7}$ and $attC_{ereA2}$ (ωB661), or *attI1* and *attI1* (ωB662, see Table S1). Integrase expression causes site-specific recombination and excision of the synthetic cassette, restoring a functional *dapA* gene and allowing these strains to grow on DAP-free medium (Figure 7A). We transformed these strains with the pBAD::*intI1* multi-copy plasmid carrying the *intI1* gene under the control of the P_{bad} promoter (p7383) and a second plasmid, p7305 (pHYD620, from (28) containing the *ssb* gene ensuring the over-expression of the SSB protein. pCL1920, the pHYD620 progenitor plasmid (p8008, devoid of *ssb* gene) was used as a control. Integrase driven recombination frequencies are calculated as the ratio of the number of cells growing in the absence of DAP over the total number of cells. Results are presented in Figure 7B.

The frequencies of excision in the absence (vector) and presence (ssb+) of SSB over-expression are significantly similar for each tested *att* combinations. These results show that SSB over-expression does not affect integron recombination.

We also tested the recombination of these three *att* combinations in the previously described *ssb-200* context (see paragraph 2, ωB769, ωB771, ωB770). For these, we constructed the MG1655Δ*dapA ssb-200* strain (ωB704, see Table S1). Results are presented in Figure 7B. Once more, excision frequencies in the *WT* and *ssb-200* strains are similar in each tested *att* combinations. These results show that SSB did not affect integron recombination.

As a control, we also performed both previously described assays in the absence of integrase expression (- IntI1, Figure 7B). We only observed a few recombination events only for the *attI1* x *attI1* reaction probably due to slippage events and/or homologous recombination between both identical 58 bp long *attI1* sites.

Effect of RecA in integron recombination

We tested the recombination of *att* sites in conditions of RecA over-expression and in a *recA* deleted mutant. Tests were performed using the previously described *in vivo* excision assay (see above). We also tested the recombination of the three previously used *att* combinations (see Materials and Methods, Table S1 and S2). The frequencies of excision in the RecA over-expression and *recA* deleted strains are significantly similar in each tested *att* combination (Figure 8). These results show that RecA does not affect integron recombination.

We also performed these assays in the absence of integrase expression (- IntI1, Figure 8). As in the SSB studies, we only observed recombination events for *attI1* x *attI1* combination, probably due to slippage events and/or homologous recombination (only in *recA*+ strain) between both *attI1* sites.

DISCUSSION

Biological functions of secondary structures

It is now obvious that DNA is not always present in its canonical double-stranded form but can also form secondary structures through intra-strand base pairing. These structures are strongly favored in single-stranded DNA and can also be extruded from dsDNA at a lower rate. These structures have been found to be involved in biological functions (15). Indeed, hairpins play an essential role in initiation of replication and transcription, and are present in a majority of origins of transfer (*oriT*) ensuring conjugation (15). Moreover, to date, there are three examples of recombination systems using secondary structures as substrates; *attC* integron recombination (9), CTX-phage integration (32) and IS*608* transposition (33). In all of the examples described above, secondary structures could represent a supplementary way to expand information storage in DNA in addition to the primary base sequence.

It is also known that too long and stable palindromes pose a threat to genome stability. Indeed, they cannot be maintained *in vivo* (for review, see (15)), either because they are inviable; i.e., intrinsically toxic to the cell or because they are genetically unstable; i.e., partially mutated or deleted (34). It is assumed that *inviability* is caused by an arrest of the replication fork, as it is unable to process these secondary structures, and *instability* is caused by the presence of proteins such as SbcCD destroying these structures. This leads to constraints on the size and perfection of the inverted repeats that can be maintained *in vivo*.

Single-strand DNA binding proteins

Hairpin formation in the cell is most likely to occur in the presence of ssDNA in the cell. The presence of ssDNA is not merely an intermediate state between its functional double-stranded forms. Indeed, ssDNA can be found in the cell during many of its physiological processes, such as lagging-strand synthesis during replication and DNA repair, but ssDNA is also tightly connected to horizontal gene exchange in bacteria, *i.e.* in bacterial conjugation, natural transformation or viral infections. When produced, cellular ssDNA is not left naked; several proteins, such as RecA and SSB, bind it without sequence specificity. The best characterized SSB is the one from the bacterium *E. coli*. SSB prevents premature annealing, stabilizes and protects the single-stranded DNA, and also removes the secondary structures (16), (17). It acts as a homotetramer that can migrate via random walk along ssDNA providing a mechanism by which it can be repositioned along ssDNA, while remaining tightly bound (18). SSB can form different complexes and bind ssDNA with several binding modes $(SSB)_n$ depending on the number of nucleotides bound per tetramer (n=35, 56 or 65). ssDNA interacts with only two SSB subunits in the $(SSB)_{35}$ complex and with all four subunits in the $(SSB)_{65}$ complex, resulting in different extents of ssDNA compaction. The binding mode defines several intertetramer cooperativities: in the $(SSB)_{35}$-binding mode, cooperativity is "unlimited" and tetramers can form long protein clusters, while in the $(SSB)_{65}$-binding mode, only dimers of tetramers (octamers) can be formed ("limited" cooperativity) (17). Moreover, SSB directs RecA binding to ssDNA and ensures the directionality of RecA polymerization across stem loop structures in ssDNA (19), (26). Indeed, the RecA protein also binds ssDNA, forming a nucleoproteic filament. Recent single-molecule studies have shown how SSB can spontaneously migrate along ssDNA, melting unstable hairpins while stimulating RecA filament elongation (18).

In this paper, we were interested in examining the role of these ssDNA-binding proteins, SSB and RecA, in integron recombination, and more specifically the role of SSB in *attC* site folding. Whereas SSB and RecA are not involved in integron recombination, we demonstrate here the involvement of SSB in the modulation of *attC* site folding in the absence of recombination.

The RecA protein does not regulate integron recombination

In order to test the effect of RecA on integron recombination, *in vivo* tests were performed by using the integron cassette excision assay where the recombination sites are carried by the chromosome. Note that we also performed supplementary tests by using our suicide

conjugation and replicative assays (data not shown). While the conjugation assay permits the delivery of *attC* sites as ssDNA, the test performed under replicative conditions supplies *attC* sites that have to be extruded as cruciforms from double strand molecules. Our results show that, whatever the delivery mode of *attC* sites, RecA does not influence integron recombination. Interesting, even RecA over-expression did not affect integron recombination. It's relevant since we know that expression of integron integrases depends on the induction of the SOS response which in turn produces a large excess of RecA. Note that this result does not exclude any regulatory role of RecA on *attC* site folding outside of recombination. Nevertheless, it seems unlikely, since previous observations showed that the RecA protein does not, by itself, bind well to ssDNA secondary structures and needs SSB to remove such structures (19).

The SSB protein modulates* attC *site folding

It was thought that SSB could have a role in integron recombination as it plays extensive cellular roles in DNA replication, DNA repair, and DNA homologous recombination, where it destabilizes secondary structures in ssDNA (25), (19), (26). Since SSB is essential for cell viability, new experimental setups were developed to study its role in integron recombination and *attC* folding. Especially, we developed a replication slippage assay using a strain with a mutated form of SSB, SSB-200, which does not hamper cell viability but confers a transposon excision phenotype (*tex*) (28). This *tex* phenotype is probably directly linked to SSB-200 not destabilizing the stem-loop structures formed by the pair of inverted repeats of the transposon. In the *ssb-200* mutated strain the frequency of reconstitution of a chloramphenicol resistance gene induced by an excision of the folded *attC* site by replication slippage is increased only in the absence of the integrase. This *in vivo* test confirmed that SSB can modify the *attC*-mediated replication slippage, probably by destabilizing the folded *attC* sites. A DNA binding assay allowed us to confirm the ability of SSB to strongly bind these sites. Note that, even if the unpaired single-stranded parts contained in the folded *attC* site (and also the unpaired derivative site) are smaller than the SSB tetramer binding site (n=35, see discussion above), SSB is able to bind to these sites. Indeed, the folded *attC* sites are probably not fixed structures and could "breathe" inducing a transient more unpaired state allowing SSB binding.

In conclusion, we demonstrated here that SSB, by "flattening" the folded *attC* sites, permits the maintenance of their integrity in the cell avoiding their deletion or mutation and also ensuring cell viability.

Stabilization constraints and recombination of hairpins

Although ssDNA is present in many contexts within the cell, hairpin formation is strongly constrained by SSB binding. Proteins that function through hairpin binding are thus in competition with SSB for substrate availability. It could be the case for the integrase since, during recombination, folded *attC* sites need to be stable enough to resist SSB melting and coating. Therefore, we proposed that the integrase could capture *attC* sites at the moment of their extrusion, efficiently stabilizing and recombining them. Here, we confirmed this hypothesis and demonstrated that, when expressed, the integrase is able to counterbalance the effect of SSB even when SSB is over expressed.

Finally, integron recombination efficiency is directed by a precise regulation of the stability of the folded *attC* sites. Bacteria have to find a subtle balance between the benefit provided by biological functions of secondary structures in DNA, and the avoidance of such structures that could be detrimental. Here, this balance seems to have been reached through the production of SSB and integrase, even though other host factors may have a role in *attC* site folding. Both proteins are capable of recognizing and acting upon these secondary structures, mediating an antagonistic effect.

We previously demonstrated the influence of cellular processes such as replication and/or horizontal gene transfer events (such as conjugation) on *attC* site folding and also the implication of superhelicity in cruciform extrusion. The multiple means of regulating *attC* site folding by the host show once again the network of cell processes that regulate integron recombination.

ACKNOWLEDGMENTS

This work was supported by the Institut Pasteur, the Centre National de la Recherche Scientifique (CNRS-UMR3525), the European Union Seventh Framework Programme (FP7-HEALTH-2011-single-stage) and the "Evolution and Transfer of Antibiotic Resistance" (EvoTAR).

The authors acknowledge Jason Bland, Dr Zeynep Baharoglu, Dr Alfonso Soler and Aleksandra Nivina for critical reading of the manuscript, and Dr Clara Frumerie for performing the EMSA quantification, and Dr Bénédicte Michel, Dr Ivan Matic and Dr Robert Lloyd for providing bacterial strains. This work is dedicated to the memory of Guy Duval-Valentin.

REFERENCES

1. **Hall RM, Collis CM.** 1998. Antibiotic resistance in gram-negative bacteria: the role of gene cassettes and integrons. Drug Resistance Updates **1:**109-119.
2. **Rowe-Magnus DA, Guerout A-M, Ploncard P, Dychinco B, Davies J, Mazel D.** 2001. The evolutionary history of chromosomal super-integrons provides an ancestry for multi-resitant integrons. P Natl Acad Sci USA **98:**652-657.
3. **Rowe-Magnus DA, Mazel D.** 2002. The Role of Integrons in Antibiotic Resistance Gene Capture. International Journal of Medical Microbiology **292:**115-125.
4. **Guerin E, Cambray G, Sanchez-Alberola N, Campoy S, Erill I, Da Re S, Gonzalez-Zorn B, Barbe J, Ploy MC, Mazel D.** 2009. The SOS response controls integron recombination. Science **324:**1034.
5. **Mazel D.** 2006. Integrons: agents of bacterial evolution. Nat Rev Microbiol **4:**608-620.
6. **Jove T, Da Re S, Denis F, Mazel D, Ploy MC.** 2010. Inverse correlation between promoter strength and excision activity in class 1 integrons. PLoS Genet **6:**e1000793.
7. **Grindley ND, Whiteson KL, Rice PA.** 2006. Mechanisms of site-specific recombination. Annu Rev Biochem **75:**567-605.
8. **Hallet B, Sherratt DJ.** 1997. Transposition and site-specific recombination: adapting DNA cut-and-paste mechanisms to a variety of genetic rearrangements. FEMS Microbiol Rev **21:**157-178.
9. **Bouvier M, Demarre G, Mazel D.** 2005. Integron cassette insertion: a recombination process involving a folded single strand substrate. Embo J **24:**4356-4367.
10. **Stokes HW, O'Gorman DB, Recchia GD, Parsekhian M, Hall RM.** 1997. Structure and function of 59-base element recombination sites associated with mobile gene cassettes. Molecular Microbiology **26:**731-745.
11. **Hall RM, Brookes DE, Stokes HW.** 1991. Site-specific insertion of genes into integrons: role of the 59-base element and determination of the recombination cross-over point. Mol Microbiol **5:**1941-1959.
12. **Bouvier M, Ducos-Galand M, Loot C, Bikard D, Mazel D.** 2009. Structural features of single-stranded integron cassette attC sites and their role in strand selection. PLoS Genet **5:**e1000632.
13. **Francia MV, Zabala JC, de la Cruz F, Garcia-Lobo JM.** 1999. The IntI1 integron integrase preferentially binds single-stranded DNA of the *attC* site. Journal of Bacteriology **181:**6844-6849.
14. **Loot C, Bikard D, Rachlin A, Mazel D.** 2010. Cellular pathways controlling integron cassette site folding. EMBO J **29:**2623-2634.

15. **Bikard D, Loot C, Baharoglu Z, Mazel D.** 2010. Folded DNA in action: hairpin formation and biological functions in prokaryotes. Microbiol Mol Biol Rev **74:**570-588.
16. **Meyer RR, Laine PS.** 1990. The single-stranded DNA-binding protein of Escherichia coli. Microbiol Rev **54:**342-380.
17. **Lohman TM, Ferrari ME.** 1994. Escherichia coli single-stranded DNA-binding protein: multiple DNA-binding modes and cooperativities. Annu Rev Biochem **63:**527-570.
18. **Roy R, Kozlov AG, Lohman TM, Ha T.** 2009. SSB protein diffusion on single-stranded DNA stimulates RecA filament formation. Nature **461:**1092-1097.
19. **Kowalczykowski SC, Krupp RA.** 1987. Effects of Escherichia coli SSB protein on the single-stranded DNA-dependent ATPase activity of Escherichia coli RecA protein. Evidence that SSB protein facilitates the binding of RecA protein to regions of secondary structure within single-stranded DNA. J Mol Biol **193:**97-113.
20. **Walker GC.** 1996. The SOS response of Escherichia coli. Escherichia coli and Salmonella. , p. 1400-1416, Neidhardt, FC Washington DC American Society of Microbiology, vol. 1.
21. **Studier FW, Rosenberg AH, Dunn JJ, Dubendorff JW.** 1990. Use of T7 RNA polymerase to direct expression of cloned genes. Methods Enzymol **185:**60-89.
22. **Johansson C, Kamali-Moghaddam M, Sundstrom L.** 2004. Integron integrase binds to bulged hairpin DNA. Nucleic Acids Res **32:**4033-4043.
23. **Demarre G, Frumerie C, Gopaul DN, Mazel D.** 2007. Identification of key structural determinants of the IntI1 integron integrase that influence attC x attI1 recombination efficiency. Nucleic Acids Res **35:**6475-6489.
24. **Frumerie C, Ducos-Galand M, Gopaul DN, Mazel D.** 2010. The relaxed requirements of the integron cleavage site allow predictable changes in integron target specificity. Nucleic Acids Res **38:**559-569.
25. **Muniyappa K, Shaner SL, Tsang SS, Radding CM.** 1984. Mechanism of the concerted action of recA protein and helix-destabilizing proteins in homologous recombination. Proc Natl Acad Sci U S A **81:**2757-2761.
26. **Reddy MS, Vaze MB, Madhusudan K, Muniyappa K.** 2000. Binding of SSB and RecA protein to DNA-containing stem loop structures: SSB ensures the polarity of RecA polymerization on single-stranded DNA. Biochemistry **39:**14250-14262.
27. **Sinden RR, Zheng GX, Brankamp RG, Allen KN.** 1991. On the deletion of inverted repeated DNA in Escherichia coli: effects of length, thermal stability, and cruciform formation in vivo. Genetics **129:**991-1005.
28. **Reddy M, Gowrishankar J.** 1997. Identification and characterization of ssb and uup mutants with increased frequency of precise excision of transposon Tn10 derivatives: nucleotide sequence of uup in Escherichia coli. J Bacteriol **179:**2892-2899.
29. **Dubois V, Debreyer C, Litvak S, Quentin C, Parissi V.** 2007. A new in vitro strand transfer assay for monitoring bacterial class 1 integron recombinase IntI1 activity. PLoS One **2:**e1315.
30. **Dubois V, Debreyer C, Quentin C, Parissi V.** 2009. In vitro recombination catalyzed by bacterial class 1 integron integrase IntI1 involves cooperative binding and specific oligomeric intermediates. PLoS One **4:**e5228.
31. **Baharoglu Z, Bikard D, Mazel D.** 2010. Conjugative DNA transfer induces the bacterial SOS response and promotes antibiotic resistance development through integron activation. PLoS Genet **6:**e1001165.

32. **Val ME, Bouvier M, Campos J, Sherratt D, Cornet F, Mazel D, Barre FX.** 2005. The single-stranded genome of phage CTX is the form used for integration into the genome of Vibrio cholerae. Mol Cell **19:**559-566.
33. **Guynet C, Hickman AB, Barabas O, Dyda F, Chandler M, Ton-Hoang B.** 2008. In vitro reconstitution of a single-stranded transposition mechanism of IS608. Mol Cell **29:**302-312.
34. **Collins J, Volckaert G, Nevers P.** 1982. Precise and nearly-precise excision of the symmetrical inverted repeats of Tn5; common features of recA-independent deletion events in Escherichia coli. Gene **19:**139-146.

Supporting information

Table S1: Bacterial strains used in this study

Table S2: Plasmids used and constructed in this study

Table S3: Oligonucleotides

FIGURE LEGENDS

Figure 1: *attC* recombination sites and a model for *attC* folding.

A) Schematic representation of a double-stranded (ds) *attC* site. Inverted repeats R'', L'', L' and R' are indicated by grey boxes. The dotted line represents the variable central part. Conserved nucleotides are indicated. Asterisks (*) show the conserved G nucleotide which corresponds to the extrahelical base (EHB) in the folded *attC* site bottom strand. Black arrow shows the cleavage point.

B) Secondary structures of $VCR_{2/1}$ and $attC_{aadA7}$ sites bottom strands (bs). Structures were determined by the UNAFOLD online interface at the Pasteur Institute. The four structural features of *attC* sites, namely, the UCS (Unpaired Central Segment), the EHB, the stem and the VTS (Variable Terminal Structure) are indicated. Black arrows show the cleavage points and asterisks, the extrahelical G bases. Primary sequences of the *attC* sites are shown (except for the VTS of the $VCR_{2/1}$ site).

C) Representation of both "ssDNA" and "dsDNA" pathways for *attC* site folding. In the "ssDNA pathway" (1, red), horizontal gene transfer (conjugation, transformation and phage infection) and replication lead to the production of ssDNA favoring *attC* hairpin formation. In the "dsDNA pathway" (2, green), an increase of supercoiling ensures cruciform extrusion. Origins of replication are shown as blue ovals and replication complexes as yellow ovals.

Figure 2: Comparison of SSB binding to several $VCR_{2/1}$ site derivatives

A) Nucleotide sequences and secondary structures of the bottom strands (bs) of $VCR_{2/1}$ site derivatives. Structures were determined by the UNAFOLD online interface at the Pasteur Institute. VCR_dbs is a VCR derivative used in EMSA experiments in which the central and imperfect part of the palindrome (VTS) was replaced by GAA. The black arrow shows the cleavage point in the R box and the asterisk (*), the extrahelical G nucleotide. We introduced mutations (bold letters) in this VCR_dbs site in order to generate, after folding, paired and unpaired (pd and unpd) VCR_dbs site derivatives. The ΔG (free energy) of VCR_dbs, pd VCR_dbs and unpd VCR_dbs folding are -21.7, -37.2 and -5.3 kcal mol^{-1} respectively.

B) EMSA analysis of the binding of SSB to $VCR_{2/1}$ site derivatives. Equal quantities of radio-labeled VCR site derivative DNA fragments (0.6pmol) were incubated with increasing amounts (0, 13, 26, 52 and 104 nM) of SSB. Complexes I and II probably represent several degrees of SSB multimerization.

C) Densitometry analysis of EMSA. Binding of SSB was measured by monitoring the fraction (×100) of the labeled DNA substrate bound by SSB in complexes I and II/labeled (bound + free) DNA, detected by automatic peak search of Image Gauge.

Figure 3: *In vivo* effect of SSB and IntI1 on *attC* site folding

A) Experimental setup of the replication slippage assay. The model proposed is that folding of the *attC* site between the pair of flanking direct repeats (EcoRI restriction sites, black rectangles) permits a replication slippage event. This results in precise or nearly precise *attC* deletion thus reconstituting a functional *cat* resistance gene (Cm^R reversion frequencies). The precise *attC* deletion is measured by sequencing (*attC* deletion frequencies).

B) SSB and IntI1 effect on Cm^R reversion and *attC* deletion frequencies (see Materials and Methods).

The replication slippage assay was used to study the IntI1Y312F and SSB effects on $attC_{aadA7}$ site folding. The Cm^R reversion frequencies and *attC* deletion frequencies are represented in the absence (-) and in the presence of IntI1 (+) in the GJ1885 wild type strain. The Cm^R reversion frequencies and *attC* deletion frequencies are represented in the GJ1885 wild type and GJ1885 *ssb-200* (GJ1890) strains. The results represent a mean of four independent experiments (see Materials and Methods). Error bars show the standard deviations.

Figure 4: Specificity of the *in vivo* effect of SSB and IntI1 on *attC* site folding

A) Secondary structures of the $attC_{aadA7}$ site bottom strand (bs) and the unpaired $attC_{aadA7}$bs site derivative. Structures were determined by the UNAFOLD online interface at the Pasteur Institute. The black arrow shows the cleavage point. Primary sequences of the *attC* sites are shown. The ΔG (free energy) of $attC_{aadA7}$bs and unpaired $attC_{aadA7}$bs folding are respectively -19.1, -5.1 kcal mol^{-1}.

B) The replication slippage assay was used to study the effect of SSB on folding of the $attC_{aadA7}$ site (black bars) and unpaired $attC_{aadA7}$ site derivative (grey bars). The relative deletion rates obtained in *ssb-200* versus GJ1885 strains (*ssb-200*/*ssb-WT*) are indicated. The results represent a mean of four independent experiments.

C) The replication slippage assay was used to study the effect of IntI1Y312F on folding of the $attC_{aadA7}$ site (black bars) and unpaired $attC_{aadA7}$ site derivative (grey bars). The relative deletion rates obtained in the presence of integrase versus in its absence (intI1+/intI1-) are indicated. The results represent a mean of four independent experiments.

Figure 5: *In vitro* effect of IntI1 on $attC_{aadA7}$ (A), $VCR_{2/1}$ (B), *attI1* (C) and $attC_{aadA7}$ *mutated* (D) site folding. The OD_{260nm} of each fragment (50 µg/ml) was measured at 37°C either after pre-chilling (pre-chilled $attC_{aadA7}$, $VCR_{2/1}$, *attI1*, $attC_{aadA7m}$), or after pre-heating for three minutes at 95°C (pre-heated $attC_{aadA7}$, $VCR_{2/1}$, *attI1* and $attC_{aadA7m}$) in the absence of IntI1, as well with the addition of IntI1 (2 pmoles) 30 min after the beginning of the measurement with pre-chilling (pre-chilled $attC_{aadA7}$ + IntI1, $VCR_{2/1}$ + IntI1, *attI1* + IntI1, $attC_{aadA7m}$ + IntI1) or after 95°C pre-heating (pre-heated $attC_{aadA7}$ + IntI1, $VCR_{2/1}$ + IntI1, *attI1* + IntI1, $attC_{aadA7m}$ + IntI1). The OD_{260nm} measurement of the proteins alone was previously performed and subtracted from the measurements obtained in the mixture in order to determine the accurate values of the ODN solution. Results represent a mean of three independent experiments. Error bars show the standard deviations.

Figure 6: *In vitro* effect of SSB on $attC_{aadA7}$ (A) and $VCR_{2/1}$ (B) site folding. The OD_{260nm} of each fragment (50 µg/ml) was measured at 37°C either after pre-chilling (pre-chilled $attC_{aadA7}$, $VCR_{2/1}$), or after pre-heating for three minutes at 95°C (pre-heated $attC_{aadA7}$, $VCR_{2/1}$) in the absence of SSB, as well as after addition of SSB (2 pmoles) 30 min after the beginning of the measurement with pre-chilling (pre-chilled $attC_{aadA7}$ + SSB, $VCR_{2/1}$ + SSB) or after 95°C pre-heating (pre-heated $attC_{aadA7}$ + SSB, $VCR_{2/1}$ + SSB). The OD_{260nm} measurement of the proteins alone was previously performed and subtracted from the measurements obtained in the mixture in order to determine the accurate values of the

fragment solution. Results represent a mean of three independent experiments. Error bars show the standard deviations.

Figure 7: *In vivo* effect of SSB on cassette excision

A) Experimental setup of cassette excision assay. The *dapA* gene is interrupted by a synthetic cassette (black line) encountered by the *attI1* (black triangle) and $attC_{aadA7}$ (white triangle) sites. The recombination leads to the excision of the integron cassette and restores a functional *dapA* gene.

B) Excision frequencies of the *attI1* x *attI1,* $attC_{aadA7}$ x $attC_{ereA2}$ and *attI1* x $attC_{aadA7}$ cassettes in WT or *ssb-200* strain (top panel) and in the presence of the pCL1920 control vector (WT) or the pHYD620 plasmid (ssb+) which over-expresses the SSB protein (bottom panel). Black bars represent the results obtained in presence of IntI1 and grey bars, in absence.
"nd" means "non-detected" recombination events. Results represent a mean of three independent experiments. Error bars show the standard deviations.

Figure 8: *In vivo* effect of RecA on cassette excision

A) Experimental setup of cassette excision assay. The *dapA* gene is interrupted by a synthetic cassette (black line) encountered by the *attI1* (black triangle) and $attC_{aadA7}$ (white triangle) sites. The recombination leads to the excision of the integron cassette and restores a functional *dapA* gene.

B) Excision frequencies of the *attI1* x *attI1,* $attC_{aadA7}$ x $attC_{ereA2}$ and *attI1* x $attC_{aadA7}$ cassettes in WT or *recA*- strain (top panel) and in the presence of the pGB2 control vector (WT) or the pGB2-recA plasmid (recA+) which over-expresses the RecA protein (bottom panel). Black bars represent the results obtained in presence of IntI1 and grey bars, in absence. "nd" means "non-detected" recombination events. Results represent a mean of three independent experiments. Error bars show the standard deviations.

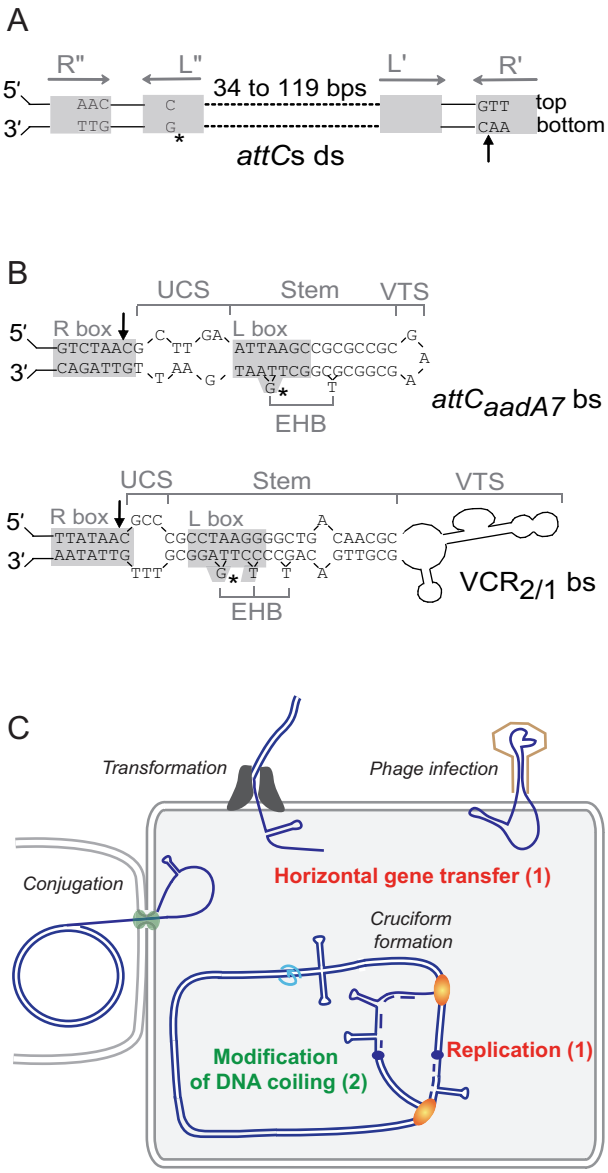
A
R"
L"
34 to 119 bps
L'
R'
5′
3′
AAC
TTG
C
G
GTT
CAA
top
bottom
attCs ds
B
UCS
Stem
VTS
R box
L box
5′
3′
GTCTAACG
CAGATTGT
ATTAAGCCGCGCCGC
TAATTCGGCGCGGCG
attC aadA7 bs
EHB
UCS
Stem
VTS
R box
L box
5′
3′
TTATAAC
AATATTG
CGCCTAAGGGGCTG
GCGGATTCCCCGAC
CAACGC
GTTGCG
VCR 2/1 bs
EHB
C
Transformation
Phage infection
Conjugation
Horizontal gene transfer (1)
Cruciform formation
Modification of DNA coiling (2)
Replication (1)

Figure 1

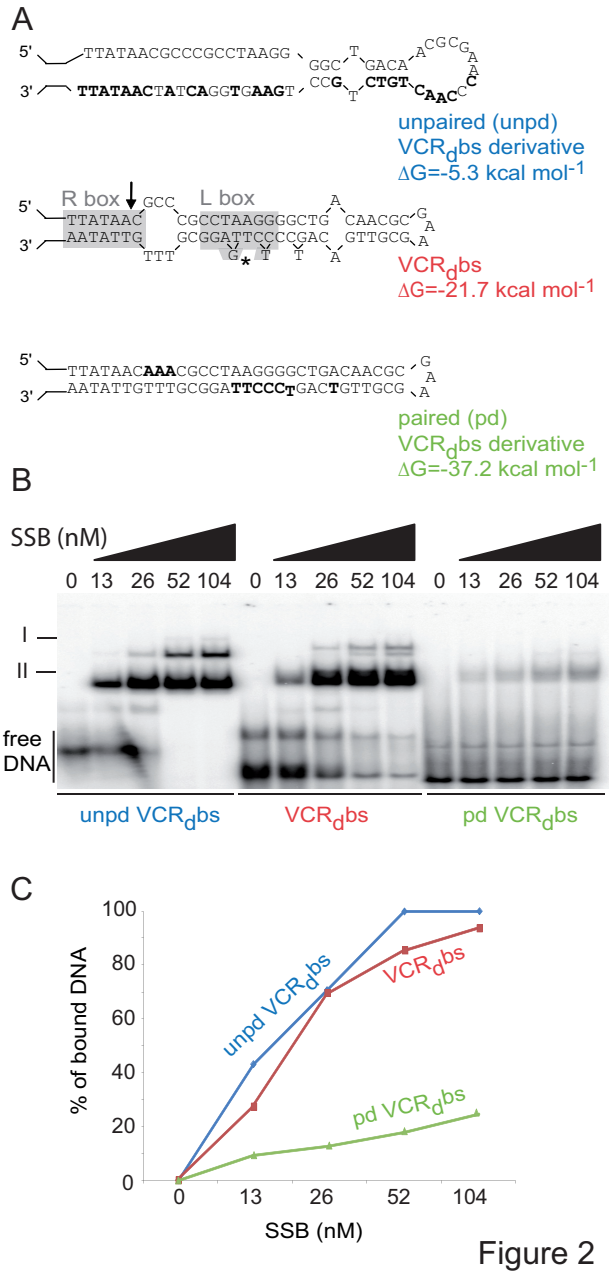
A
unpaired (unpd)
VCRdbs derivative
ΔG=-5.3 kcal mol-1
R box
L box
VCRdbs
ΔG=-21.7 kcal mol-1
paired (pd)
VCRdbs derivative
ΔG=-37.2 kcal mol-1
B
SSB (nM)
0 13 26 52 104 0 13 26 52 104 0 13 26 52 104
I
II
free DNA
unpd VCRdbs
VCRdbs
pd VCRdbs
C
% of bound DNA
100
80
60
40
20
0
0 13 26 52 104
SSB (nM)
unpd VCRdbs
VCRdbs
pd VCRdbs

Figure 2

A

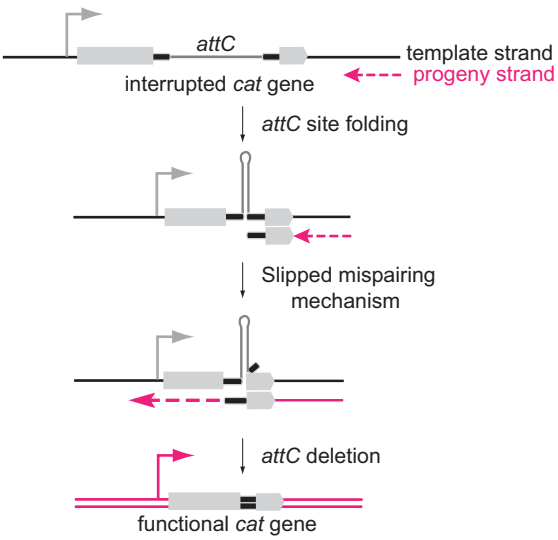

B

Strains	*intI1* expression	Cm^R reversion frequencies	*attC* deletion frequencies
GJ1885	-	5.5×10^{-11} +/- 2.3×10^{-11}	5.5×10^{-11}
	+	1.4×10^{-9} +/- 5.7×10^{-10}	1.4×10^{-9}
ssb-200	-	7.6×10^{-10} +/- 1.5×10^{-10}	7.6×10^{-10}
	+	1.3×10^{-9} +/- 2.0×10^{-10}	8.7×10^{-10}

Figure 3

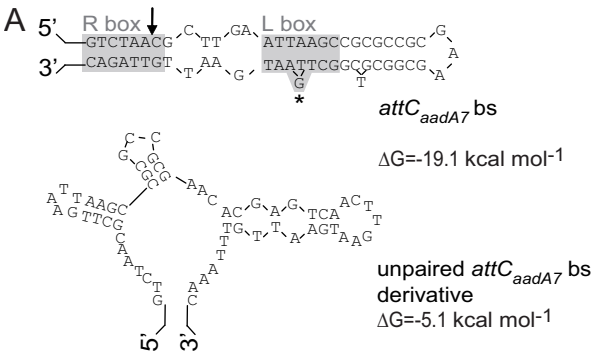
A
5'
3'
R box
L box
GTCTAACG
CAGATTGT
ATTAAGCCGCGCCGC
TAATTCGGCGCGGCG
*
attC aadA7 bs
ΔG=-19.1 kcal mol-1
unpaired attC aadA7 bs derivative
ΔG=-5.1 kcal mol-1
5'
3'

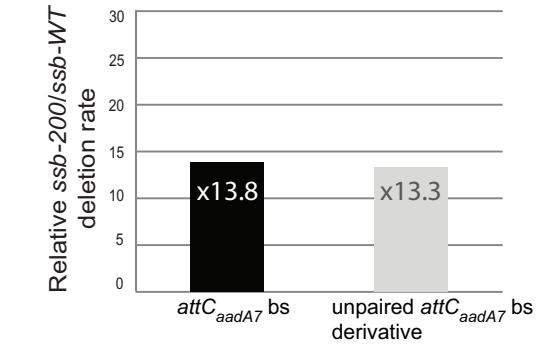
B
Relative ssb-200/ssb-WT deletion rate
30
25
20
15
10
5
0
x13.8
x13.3
attC aadA7 bs
unpaired attC aadA7 bs derivative

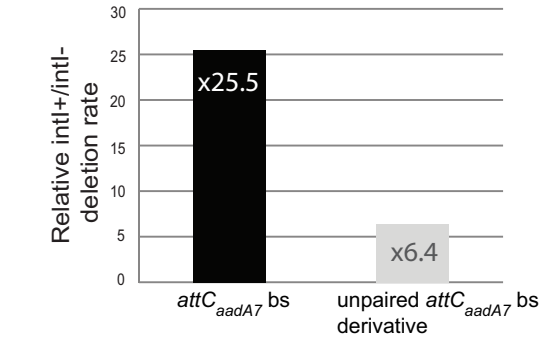
C
Relative intI+/intI- deletion rate
30
25
20
15
10
5
0
x25.5
x6.4
attC aadA7 bs
unpaired attC aadA7 bs derivative

Figure 4

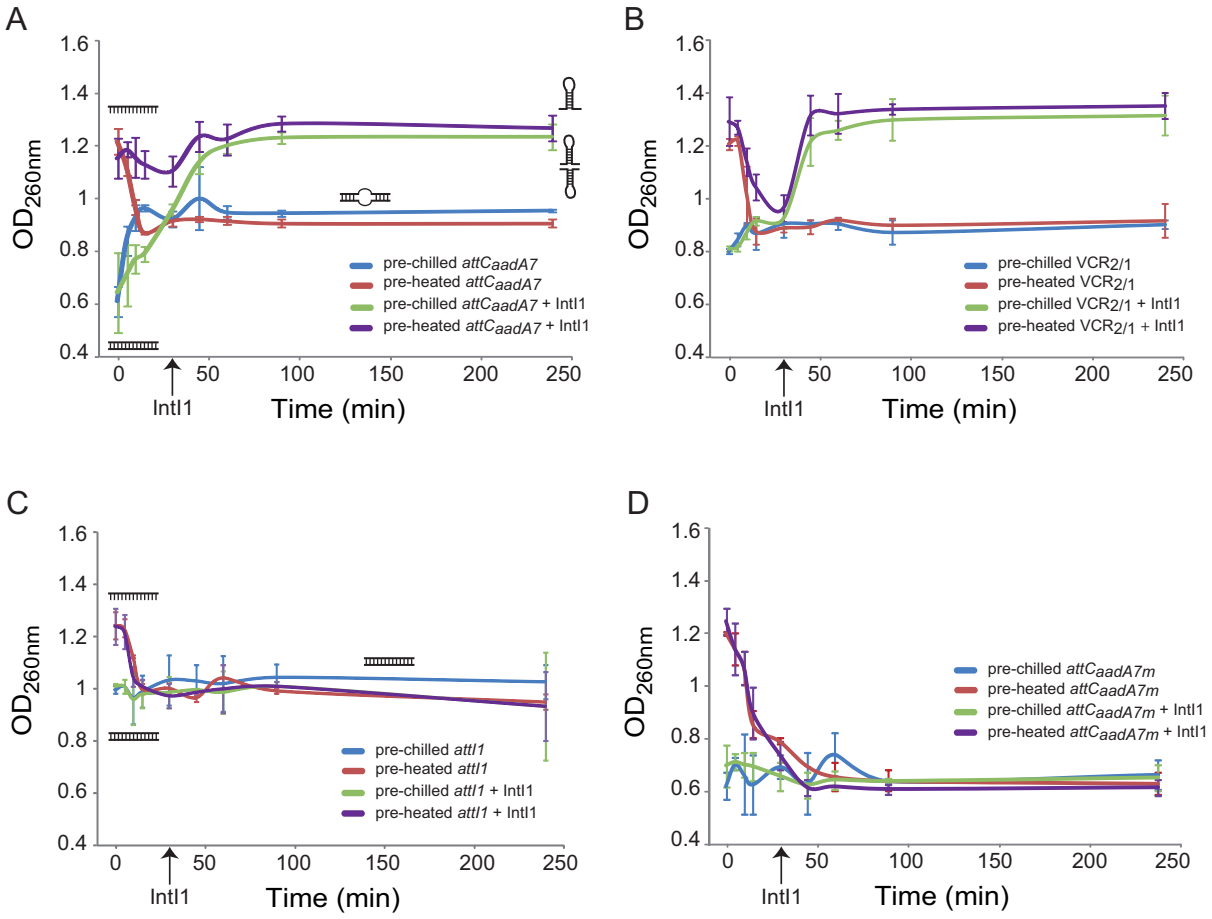
A
B
C
D
OD260nm
Time (min)
IntI1
pre-chilled attCaadA7
pre-heated attCaadA7
pre-chilled attCaadA7 + IntI1
pre-heated attCaadA7 + IntI1
pre-chilled VCR2/1
pre-heated VCR2/1
pre-chilled VCR2/1 + IntI1
pre-heated VCR2/1 + IntI1
pre-chilled attI1
pre-heated attI1
pre-chilled attI1 + IntI1
pre-heated attI1 + IntI1
pre-chilled attCaadA7m
pre-heated attCaadA7m
pre-chilled attCaadA7m + IntI1
pre-heated attCaadA7m + IntI1

Figure 5

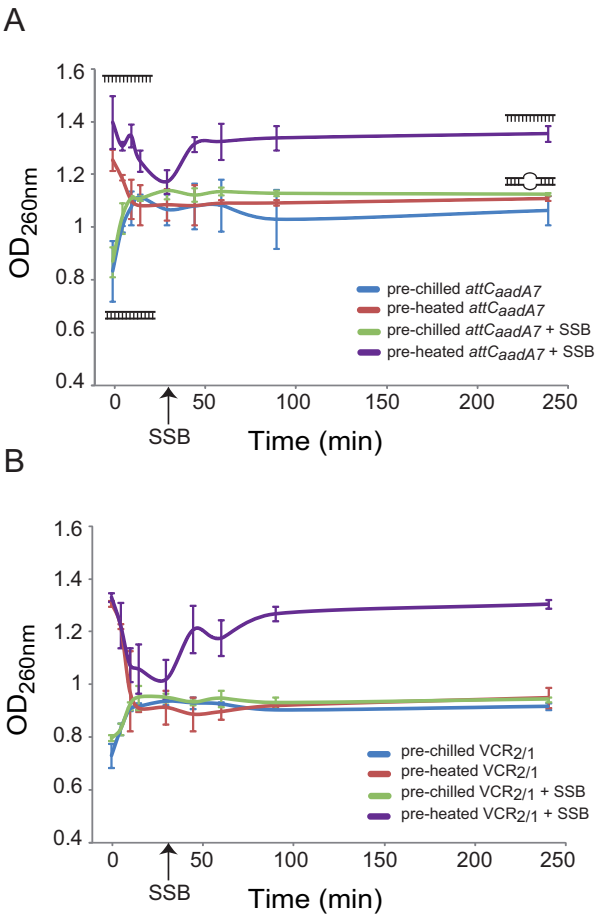
A
1.6
1.4
1.2
1
0.8
0.6
0.4
OD260nm
0
50
100
150
200
250
SSB
Time (min)
pre-chilled attCaadA7
pre-heated attCaadA7
pre-chilled attCaadA7 + SSB
pre-heated attCaadA7 + SSB
B
1.6
1.4
1.2
1
0.8
0.6
0.4
OD260nm
0
50
100
150
200
250
SSB
Time (min)
pre-chilled VCR2/1
pre-heated VCR2/1
pre-chilled VCR2/1 + SSB
pre-heated VCR2/1 + SSB

Figure 6

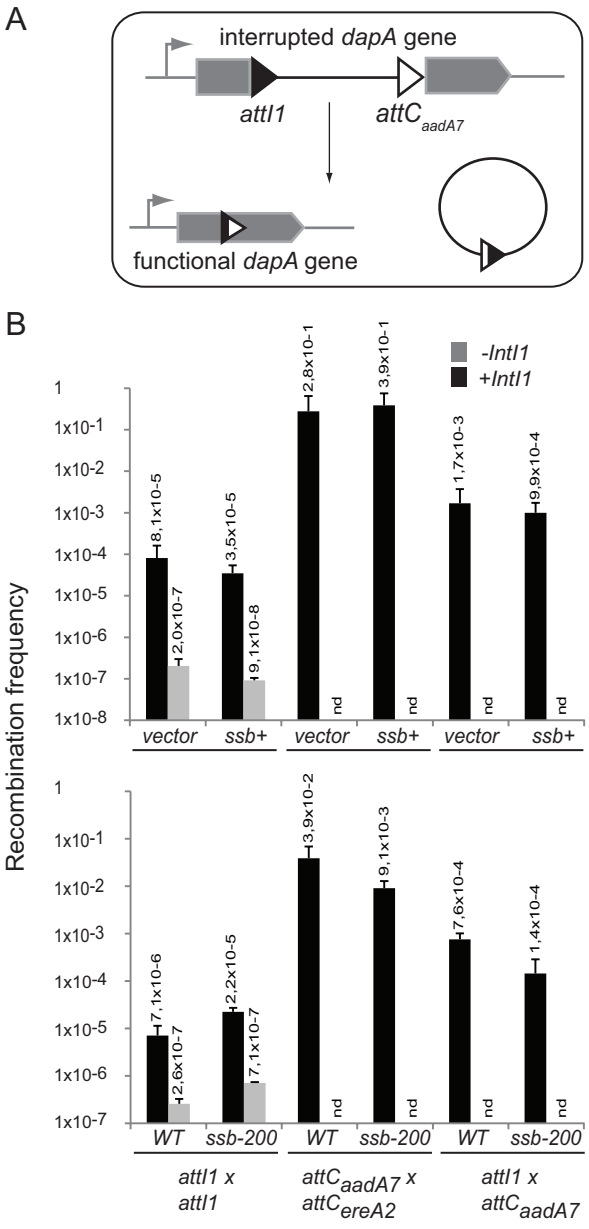
A
interrupted dapA gene
attI1
attC aadA7
functional dapA gene
B
-IntI1
+IntI1
Recombination frequency
1
1x10-1
1x10-2
1x10-3
1x10-4
1x10-5
1x10-6
1x10-7
1x10-8
8,1x10-5
2,0x10-7
3,5x10-5
9,1x10-8
2,8x10-1
3,9x10-1
1,7x10-3
9,9x10-4
nd
vector
ssb+
7,1x10-6
2,6x10-7
2,2x10-5
7,1x10-7
3,9x10-2
9,1x10-3
7,6x10-4
1,4x10-4
WT
ssb-200
attI1 x attI1
attC aadA7 x attC ereA2
attI1 x attC aadA7

Figure 7

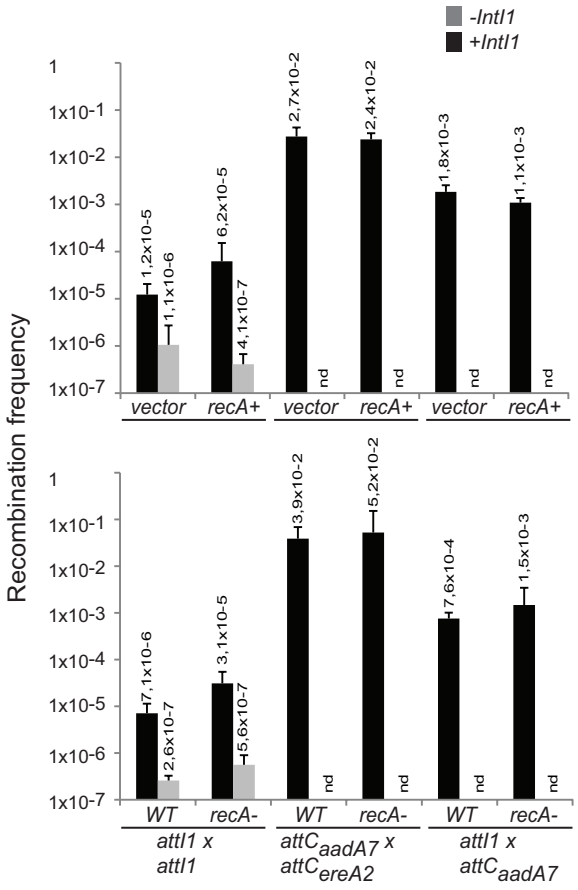
-IntI1
+IntI1
Recombination frequency
1
1x10-1
1x10-2
1x10-3
1x10-4
1x10-5
1x10-6
1x10-7
1,2x10-5
1,1x10-6
6,2x10-5
4,1x10-7
2,7x10-2
nd
2,4x10-2
nd
1,8x10-3
nd
1,1x10-3
nd
vector
recA+
vector
recA+
vector
recA+
7,1x10-6
2,6x10-7
3,1x10-5
5,6x10-7
3,9x10-2
nd
5,2x10-2
nd
7,6x10-4
nd
1,5x10-3
nd
WT
recA-
WT
recA-
WT
recA-
attI1 x attI1
attC aadA7 x attC ereA2
attI1 x attC aadA7

Figure 8